Science of the Total Environment 811 (2022) 152172

Contents lists available at ScienceDirect

Science of the Total Environment

journal homepage: www.elsevier.com/locate/scitotenv

Factors dominating the horizontal and vertical variability of soil water vary with climate and plant type in loess deposits

Yanan Huang [a], Bingbing Li [a], Asim Biswas [b], Zhi Li [a,*]

[a] College of Natural Resources and Environment, Northwest A&F University, Yangling, Shaanxi 712100, China
[b] School of Environmental Sciences, University of Guelph, Guelph, Ontario N1G 2W1, Canada

HIGHLIGHTS

- Soil water variability was explored with a large dataset under varying environment.
- Soil water varies horizontally and vertically with changing environmental factors.
- Plant age and soil clay content dominate horizontal variability of soil water.
- Plant age and NDVI dominate vertical variability of soil water.
- Dominance of vegetation highlight impacts of deep-rooted plants.

GRAPHICAL ABSTRACT

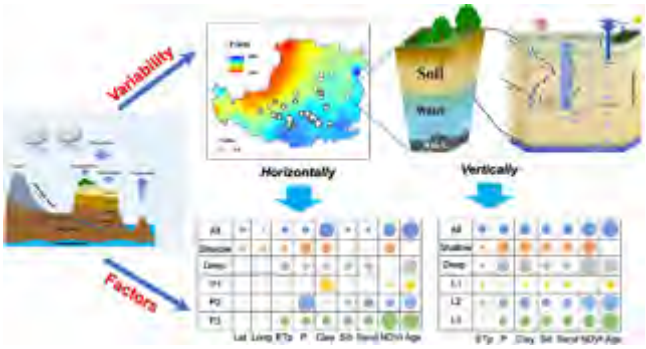

ARTICLE INFO

Article history:
Received 16 June 2021
Received in revised form 28 November 2021
Accepted 30 November 2021
Available online 6 December 2021

Editor: Paulo Pereira

Keywords:
Soil water
Spatial variability
Deep-rooted plant
Dominant factor
Multimodel inference method

ABSTRACT

Identifying the variability and predominant factors affecting soil water (SW) is essential in regions with thick vadose zones and deep-rooted plants. This information is needed to clarify the balance between water availability and plant water demand. We collected 9263 soil samples from 128 profiles of 7–25 m deep soil under different climates (arid, semiarid and subhumid), soil textures and plant types (shallow or deep roots) in China's Loess Plateau. The factors dominating the horizontal and vertical variability of SW were identified using a multimodel inference approach and stepwise regression analysis. Horizontally, the mean water content and storage increased while the water deficits decreased from the northwest to the southeast. Vertically, mean water content and storage are highest in the relatively stable layer, followed by rapidly changing layers and active layers. Plant age and soil clay content dominate the horizontally varied SW, while plant age and normalized difference vegetation index (NDVI) dominate the vertical variability of SW. However, the dominant factors appeared to differ with climate and plant type. It was determined that for climate, soil clay content and plant age in arid regions, precipitation and plant age in semiarid regions, NDVI and plant age in subhumid regions were important factors. For plants, the dominant factors are NDVI and precipitation under shallow-rooted plants; however, NDVI and plant age were dominant under deep-rooted plants. The dominance of plant age highlighted the impact of vegetation patterns on SW, especially for deep-rooted plants, which should be taken into account when managing water resources and ecosystem rehabilitation in degraded regions.

1. Introduction

Soil water (SW) is a critical factor limiting the eco-environmental development in arid agroforestry systems and it directly determines the vegetation carrying capacity together with its reallocation patterns (Jian et al., 2015; Rodriguez-Iturbe et al., 1999). Plants, in turn, transport SW to the atmosphere via the root system (Zhang and Wei, 2021). These processes exhibit complex horizontal and/or vertical variability which is

* Corresponding author.
E-mail address: lizhibox@nwafu.edu.cn (Z. Li).

http://dx.doi.org/10.1016/j.scitotenv.2021.152172

affected by geographical features (Hu and Si, 2014), climate (Perry and Niemann, 2007; Wilson et al., 2005), soil type (Namdar-Khojasteh et al., 2012), vegetation (Bosch et al., 2006; Li and Huang, 2008) and their interactions at different scales (Chen et al., 2008; da Silva et al., 2001; Dekker et al., 2007; Hu and Si, 2013). As such, understanding the variability and controlling factors affecting SW is important for the optimal management and sustainability of ecosystems.

The variability in SW results in different interactions between soils, climate and plants, and can affect the patterns of vegetation succession and terrestrial carbon uptake (Gao and Shao, 2012; Green et al., 2019; Guillod et al., 2015; Western et al., 2004; Zhang et al., 2016). Previous studies mainly discussed the horizontal variability of SW in surface layers from in situ measurements, remote sensing or reanalysis data (Bosch et al., 2006; Famiglietti et al., 1998; Feng et al., 2017; Gao et al., 2016; Melliger and Niemann, 2010; Petropoulos et al., 2015). However, little is known about how environmental factors influence SW stored in deep layers. In particular, the vertical variability of SW requires further investigation due to the lack of climate and vegetation data. This is the case in regions with complex vegetated structures and variable water storage in different layers, all of these changes interact with the plant root systems and the impact of climate. Thus, a detailed investigation is needed to understand the requirements for water sustainability.

The variability and controlling factors of SW have been investigated previously, but these studies provide conflicting conclusions. As an example of this, global microwave satellite observations from 1998 to 2008 indicated that the interaction of soil moisture and evapotranspiration largely reveal the mechanism of land-evapotranspiration decline at the global scale (Jung et al., 2010). In contrast, total precipitation during the plant's growing season was found to be the most important factor controlling soil water storage on the loess hillslopes (Mei et al., 2019). However, a meta-analysis of 1262 SW data within 0–5 m in three ecological zones suggested SW was controlled by temperature rather than precipitation on the Loess Plateau (Su and Shangguan, 2019). There may be several explanations for the differing results. First, the factors controlling SW are variable including climate such as rainfall or evapotranspiration (Cleverly et al., 2016), terrains such as gully or hillslope (Famiglietti et al., 1998; Gao et al., 2016), soils (Hendrickx et al., 1990; Qu et al., 2015) and land use patterns (Stonestrom et al., 2009; Ziadat and Taimeh, 2013). Second, data size influences the reliability of the results. Third, the methods used for factor identification may produce diversified results (da Silva et al., 2001; Qiao et al., 2018; Sándor et al., 2021). As such, large datasets and appropriate methods are very important to identify the dominant factors to fully understand the variability of SW.

To identify the factors controlling SW, several multivariate analysis techniques have been employed, e.g., principal component analysis and canonical correlation analysis (Shao et al., 2009; ter Braak and Verdonschot, 1995). Further, to eliminate the multicollinearity of the selected factors, a stepwise multiple linear regression has been used to explain the relative importance of the variables (Maddock, 1976; Sun et al., 1998). However, if only one combination of factors is identified, it may fail to take into account other combinations with good predictive performance. As an alternative, the multimodel inference approach compares many models by conducting an exhaustive search (Duan et al., 2007; Mohan et al., 2018; Poeter and Anderson, 2005). As such, combining different methods offers a good perspective on identifying the dominant factors of SW variability.

The loess deposits in the Loess Plateau have stored information about past climate and soil formation, which may complicate the vertical variability of soil characteristics (Tite and Linington, 1975; Vidic et al., 2004). It has arid, semiarid and subhumid climates changing successively from northwest to southeast; the soil is also diverse (Gong and Zhang, 2007; Zhu et al., 1983). In addition, since 1999, the vegetation restoration related projects have returned many steep cultivated farmlands to forests and grasslands (An et al., 2017; Yao et al., 2016). This change has greatly influenced the SW reservoirs (Feng et al., 2016; Jiao et al., 2016). The Loess Plateau has become an important site for ecohydrology. Considering the complicated natural variability and anthropogenic impacts, exploring the variability and dominant factors of SW increases the predictability of deep SW and provides better information for understanding regional SW patterns and managing water resources.

In this study, we analyze unusually-deep SW contents datasets from 9263 soil samples at multiple locations including different climates, soils and vegetations in the Loess Plateau to explore the SW variability. We also relate vertical SW at different depths with historical precipitation to enlarge the datasets. With them, we address the following questions: (1) What is the horizontal and vertical variability of SW? (2) How do the environmental factors affect SW variability? (3) Why the SW variability is different under shallow- and deep-rooted plants? Furthermore, we develop the predicted models of SW based on the dominant factors. The results can be used to understand soil hydrology and manage SW resources in deep vadose zones.

2. Materials and methods

2.1. Study area

The Loess Plateau, located in the middle reach of the Yellow River Basin, has an area of 6.2×10^5 km^2 (Fig. 1a). The precipitation ranges from 140 to 680 mm along the northwest-southeast direction, 55–78% of which is concentrated from June to September as heavy rainfall. The evaporation and temperature range 1400–2000 mm and 3.6–14.3 °C from the northwest to the southeast, respectively (Shi and Shao, 2000). The soil is characterized by a strong zonal distribution with coarse sandy soil in the northwest and finer clayey soil in the southeast (Gong and Zhang, 2007; Zhu et al., 1983). The loess deposits, vertically, have stratification and differentiation. With low vegetation cover, steep slopes, intensive rainfall and erodible loess, the Loess Plateau has suffered severe soil erosion in the past several decades (Biggelaar et al., 2003; Lal, 2001). Since the 1950s, several afforestation plans have been implemented to control soil loss (Jing et al., 2013). The artificial woodlands include apple (*Malus pumila* Mill.), poplar (*Populus* L.), jujube (*Ziziphus jujuba* Mill.), Chinese pine (*Pinus tabuliformis* Carr.), apricot (*Armeniaca sibirica* L.), while the shrublands include sea buckthorn (*Hippophae rhamnoides* L.), caragana microphylla (*Caragana korshinskii* Kom.) and salix mongolica (*Salix cheilophila*). The land use types in this study mainly cover artificial woodland, shrubland and farmland.

2.2. Data description

2.2.1. Soil water

SW profiles were collected at different locations taking into consideration variable climates, soils and vegetation. Overall, 128 soil profiles were sampled between April 2001 and September 2018 (Fig. 1); these were either sampled for this study (39 profiles) or collected from the literature (89 profiles). With depths of 7–25 m, 9263 soil samples were collected to determine water content. The gravimetric water content was determined by the oven drying method at an interval of 20 cm. To consider the impact of plants, at each location, we collected soil samples to the same maximum depth for shallow- and deep-rooted plants. Specifically, shallow-rooted plants (root length < 2 m) include farmlands with wheat, maize or grasslands, while deep-rooted plants (root length > 2 m), with various growing ages ranging from 3 to 70 years old, include trees (e.g., apple, apricot, peach, poplar, *Juglans regia*, quercus wutaishanica, *Platycladus orientalis*, *Pinus tabuliformis*, salix mongolica, jujube), shrubs (e.g., *Sophora davidii*, locust forest, sea buckthorn, caragana), deep-rooted herbage (i.e. alfalfa) and some intercropping lands of them. At the same location, the distance between sites with different plants is <100 m to ensure similar soil and climate characteristics.

The sampling sites have mean annual precipitation of 185 to 622 mm (Table S1). Among them, 6, 16 and 106 profiles were collected in regions with mean annual precipitation 0–200 mm (P1, arid climate), 200–400 mm (P2, semiarid climate) and 400–800 mm (P3, subhumid climate), respectively. The profiles are located in regions with different soil

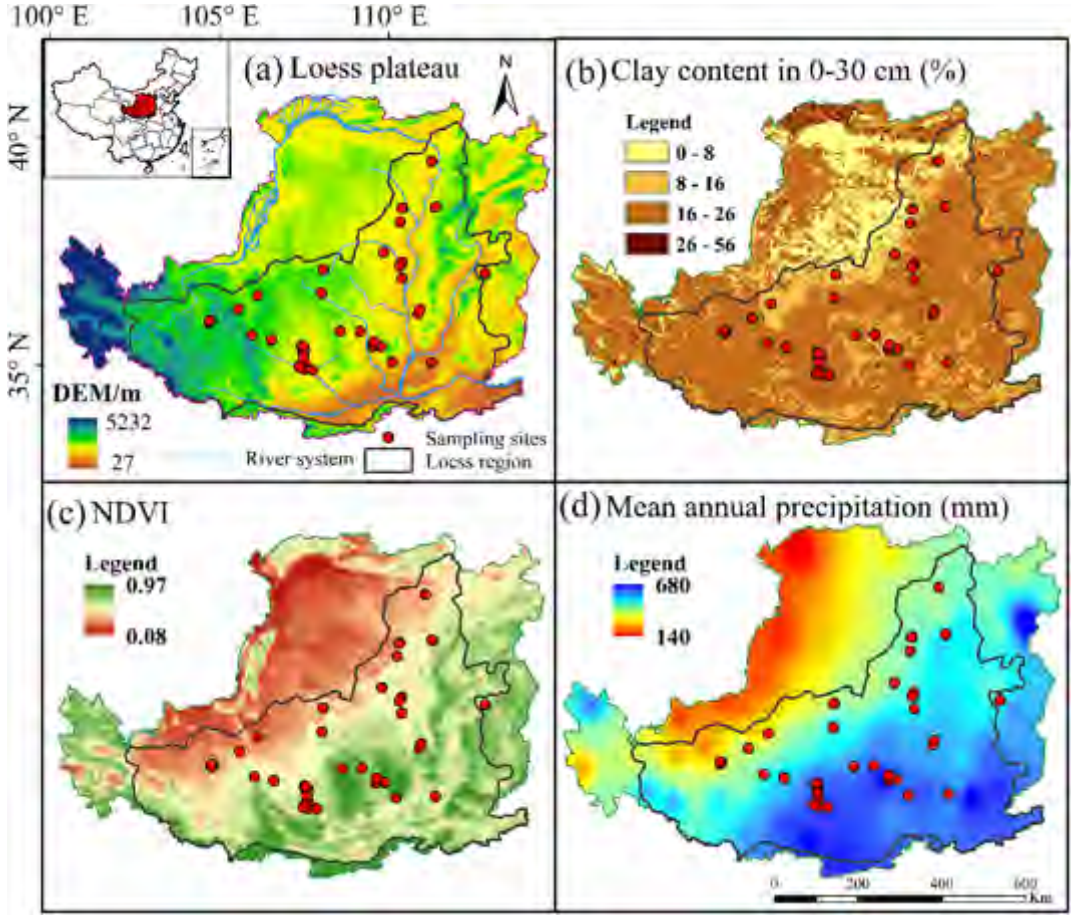

Fig. 1. Sampling sites and environmental conditions of the Loess Plateau. (a) Digital Elevation Model (DEM). (b) Averaged soil clay content in 0–30 cm. (c) Normalized Difference Vegetation Index (NDVI) in 2015. (d) Mean annual precipitation during 1956–2017.

conditions with mean soil clay content ranging from 10.2% to 27.7%. For vegetation, 47 and 81 profiles were collected under shallow- and deep-rooted plants, respectively. The diverse climates, soils and vegetation provide a large dataset to analyze the controlling factors of SW variability.

Besides the measured soil water content, two indicators will be used, i.e., soil water storage (SWS) and soil water deficit (WD). SWS reveals the actual amount of water stored in the profile, which may reflect the combined effects of climate, soil and root systems; *WD* indicates how much water has been consumed by plants or moved away by other processes (Grassini et al., 2010; Wang et al., 2015).

$$SWS = SW \times SBD \times h \times UFC/\rho \quad (1)$$

$$WD = WHC - SWS \quad (2)$$

where *SW* is soil water content (%); *SBD* is soil bulk density (g cm^{-3}); ρ is density of SW (g cm^{-3}); *WHC* is water holding capacity (-0.03 MPa) (%); *UFC* is a unit conversion factor (10 mm cm^{-1}); *h* is soil thickness (mm). The above indicators were estimated for each layer or the whole profile.

2.2.2. Environmental factors

To analyze the controlling factors of SW variability, we determined or collected data related to climate (precipitation P, and potential evapotranspiration ET_p), soil texture (Clay, Silt, and Sand), vegetation (Normalized Difference Vegetation Index NDVI, and plant age Age) and geography (latitude Lat, and longitude Long). Time series of climate data were collected from a 1-km monthly precipitation and temperature dataset for the period 1901–2017 (Peng et al., 2019). ET_p was estimated by the Hargreaves formula with temperature data (Hargreaves, 1994; Jensen et al., 1997). For soil, profiles of soil texture and water tritium content were either obtained by this study or collected from the literature. Soil textures were measured by the international pipette method (Piper, 1966), while the tritium content, extracted from fresh soil using a vacuum condensation extraction system, was determined by a Low-background Liquid Scintillation Counter (Quantulus 1220, PerkinElmer, Singapore). For vegetation, the ages of shallow-rooted plants were set as one year old, while the various ages of deep-rooted plants can be used to show indirectly the impact of root systems since plant ages are positively correlated with root density (Li et al., 2018; Li et al., 2019a). Additionally, we extracted NDVI for each sampling site from the aqua MODIS vegetation indices (MYD13Q1) version 6 of 250-m resolution to reflect the vegetation conditions (https://lpdaac.usgs.gov/). For geographical factors, longitude and latitude were used to explore the potential impact of water and energy, respectively. The slope was not considered as a geographical factor because most sampling sites had flat surfaces except for three sites (QJ, WQ and SD).

2.3. Analyzing soil water variability

The horizontal variability of SW was analyzed by showing the spatial pattern of water content averaged across each soil profile, which can be used to link SW content to climate, soil, vegetation and other factors at large scale. In particular, we compared the SW under shallow- and deep-rooted plants to show the effects of vegetation, and compared the SW in different climatic regions to explore the control of climate on horizontal variability.

For the vertical variability of SW, the whole soil profile will be grouped into three soil layers: rapidly changing layer (frequent conversion between

wet and dry, greatly affected by rainfall and evaporation), active layer (water consumption layer, mainly affected by microclimate and root system) and relatively stable layer (minor change, affected little by external conditions) (Li et al., 2020). The three layers were partitioned with the standard deviation and variation coefficient of SW changes. Similarly, the analysis of vertical variability was conducted for all sites, sites with shallow- or deep-rooted plants, sites with different climates to explore the effects of vegetation or climate.

To quantify the variability, the coefficient of variation (CV) was employed. In general, CV of 0–0.1, 0.1–1, and >1 suggest low, moderate and high variations, respectively (Glüer et al., 1995; Nielsen et al., 1973; Sandrin et al., 2003). Further, the significance of the difference in SW content was evaluated by analysis of variance (ANOVA, $p = 0.05$).

2.4. Identifying controlling factors

The controlling factors were explored by linking SW indicators with climate, soil texture, vegetation and geography in the horizontal or vertical direction. In the horizontal direction, the SW indicators averaged for the whole profile can be directly correlated with the above mentioned environmental factors. In the vertical direction, the profiles were divided into two groups, i.e., shallow-rooted plants and deep-rooted plants.

Under shallow-rooted plants, the SW profiles are influenced less by the root system, but are more easily affected by soil and climate. The soil texture can be directly determined at each depth, but the climate-soil relationship in the vertical direction should be established. If SW moves downward in the form of piston flow, the SW at different depths may be the result of precipitation in different years. With SW tritium profiles, the ages of SW at different depths can be approximated by the tritium peak method (Fig. 2). Specifically, the infiltration rate of SW is estimated first as the tritium peak depth divided by the years from 1963 to sampling year. Then, SW age in each layer can be inversely estimated according to the depth and infiltration rate. This method is feasible in the study area since the water moves in the form of piston flow revealed by tritium and other tracer profiles (Allison and Hughes, 1978; Li et al., 2019b). As such, the relationship between SW and soil texture/historical precipitation can be explored at different depths. This procedure actually extends the SW data in the vertical direction to a long-term dynamic monitoring dataset, which provides more data for analysis of rainfall infiltration conditions.

Under deep-rooted plants, the vertical variability of SW is small because of excessive root water uptake (Beyer et al., 2018; Bleby et al., 2010; Cui et al., 2019; Markewitz et al., 2010), which can be seen from later data. Except for the factors considered for shallow-rooted plants, we also explored the effects of plant age.

For both the horizontal and vertical directions, three steps were conducted to identify the factors dominating SW variability. First, the Pearson correlation coefficient was used to determine the preliminary importance of each factor. Simultaneously, each factor was solely regressed against the compiled SW, and the factors were selected based on the coefficient of determination (R^2), root-mean-square error (RMSE) or significance ($p = 0.05$). This step eliminated the least influential factors for subsequent analysis. Second, the least square stepwise regression was conducted for the identified factors to present a series of regression models. Based on an exhaustive

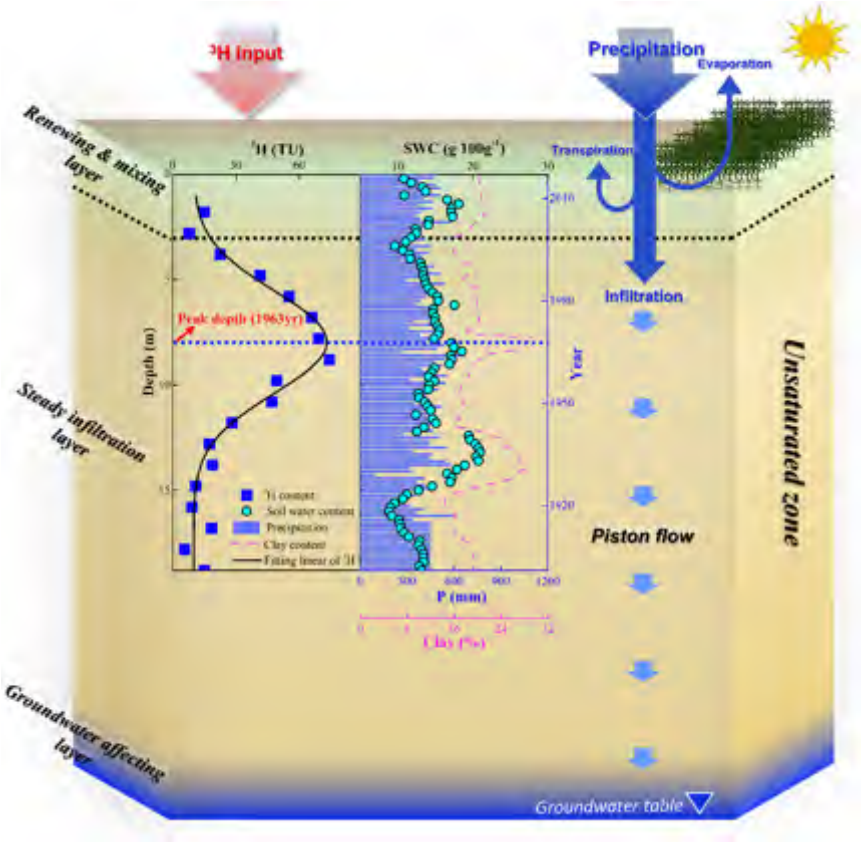

Fig. 2. Conceptual model for water movement of piston flow revealed by tritium (blue quadrate) in the unsaturated zone, including reviewing and mixing layer, steady infiltration later, and groundwater affecting layer. The 'bomb peak' clearly records the maximum tritium concentrations associated with precipitation ~1963 (blue dotted line). SW contents above and below the peak depth mainly refer to the 'modern water' (after 1963) and 'old water' (before 1963), respectively. Further, the ages of SW in the different soil layers were also defined by the tritium peak method, which is consistent one-to-one match with precipitation (blue pillar) and soil clay content (red dotted line). (For interpretation of the references to colour in this figure legend, the reader is referred to the web version of this article.)

search, all candidate models were fitted and inter-compared (Fenicia et al., 2008; Mohan et al., 2018). The performance evaluation criteria R^2 was used to ascertain the optimal model; the reasonableness of this model was evaluated by residual analysis. To exclude the potential multicollinearity between two or more factors, we used the variance inflation factor (*VIF*) and tolerance ($1\text{-}R_i^2$) to conjointly verify multicollinearity. A *VIF* smaller than 10 or a tolerance greater than 0.2 suggests negligible multicollinearity among the influencing factors. Third, the proportion of evidence (PoE, 0–1), i.e., the weighted sum of all the models containing a certain factor, was employed to select the most important factors. A PoE closer to 1 suggests a greater impact. To clarify the effect of environmental factors on SW, we focused on the top two identified dominant factors.

2.5. Predicting SW models

With the identified factors and regressed equations, is it possible to predict SW without direct measurement? We randomly split the dataset into two groups, i.e., 80% of the data for model development and 20% of the data for model validation. The evaluation of the models was improved by splitting the datasets 1000 times to decrease the uncertainties and improve the accuracy of predicted models. Multimodel inference analysis improves model performance by introducing one variable at a time, and then, the model with satisfactory performance (R^2 and RMSE) can be chosen (Mohan et al., 2018).

All statistical analyses were performed with Microsoft Excel 2019, SPSS 22.0, and MATLAB R2017b. All graphs were generated with GIS

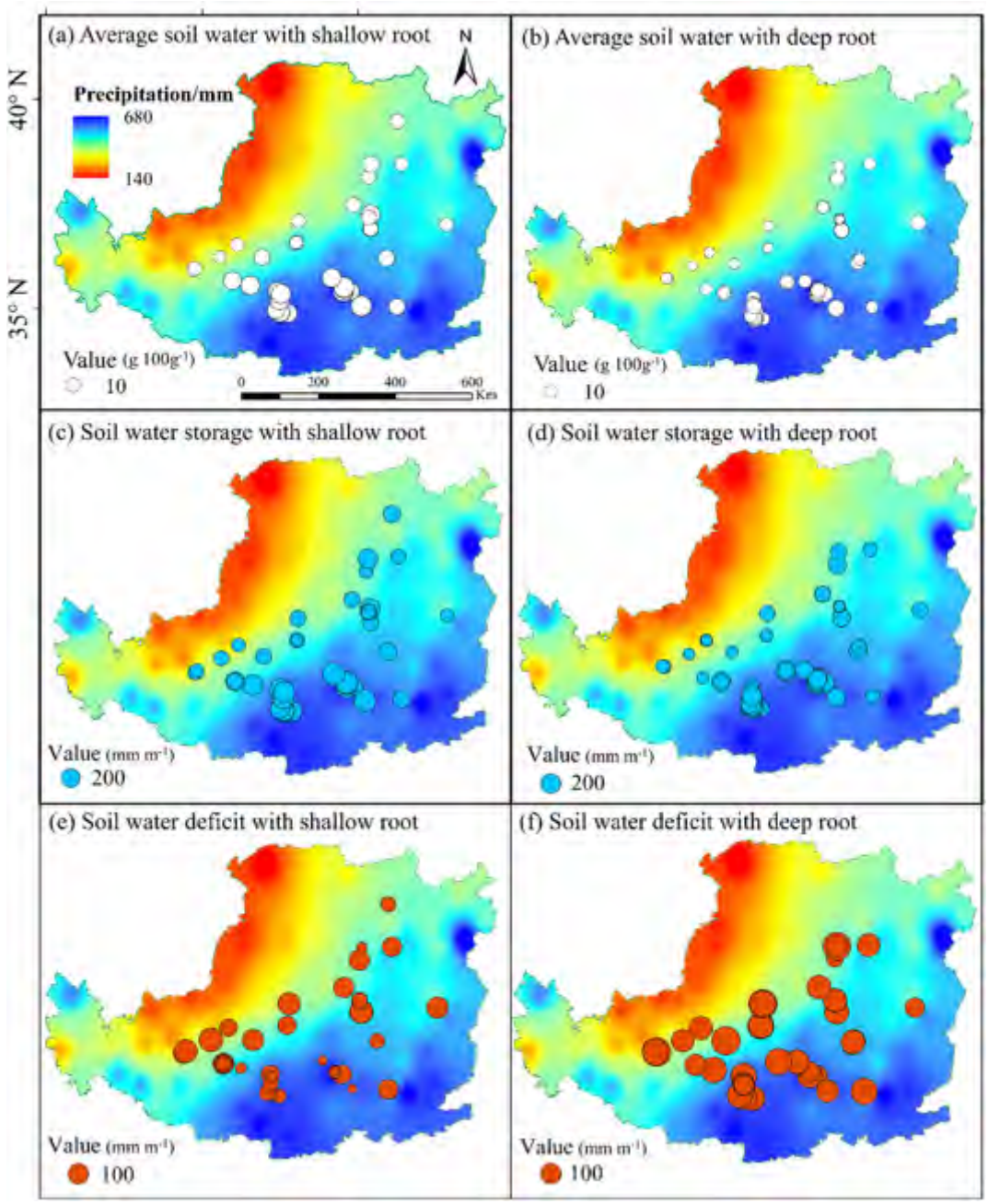

Fig. 3. Spatial patterns in soil water indicators. (a–b) Mean soil water content of each site. (c–d) Soil water storage of each site in per meter. (e–f) Soil water deficit of each site in per meter. The white, blue and red circles with different sizes refer to the value of soil water content, storage and deficit, respectively. 10, 200 and 100 represent the value of averaged soil water, storage and deficit in per meter corresponding to related bubble sizes, respectively. (For interpretation of the references to colour in this figure legend, the reader is referred to the web version of this article.)

software (ESRI® ArcMap™ 10.5), OriginPro 2016 and Microsoft PowerPoint 2016.

3. Results

3.1. Horizontal variability of SW

To investigate the horizontal variability of SW, we presented the spatial patterns of the mean SW content as well as the storage and deficit in each soil profile (Fig. 3). The SW indices have large horizontal variability since the mean SW content, storage and deficit range from 5.0–21.1 g 100 g^{-1}, 63–308 mm m^{-1}, and − 32–195 mm m^{-1}, respectively (Table 1). But most SW indices spatially vary with gradients along the northwest-southeast direction. Regardless of plant type, SW content and storage increase from the northwest to the southeast. However, water deficit has spatial patterns varying with plant type, and it decreases with shallow-rooted plants with little difference with deep-rooted plants along the northwest-southeast direction.

The overall spatial patterns of SW indices appear consistent with that of precipitation, which may reflect the impact of climate. For example, the mean SW content is at its highest in the subhumid climate (13.0 ± 4.4 g 100 g^{-1}), intermediate for the semiarid climate (9.3 ± 4.1 g 100 g^{-1}), and the lowest for arid climate (8.6 ± 1.8 g 100 g^{-1}) (Table 1). With different plants, SW content and storage under shallow-rooted plants are greater than those under deep-rooted plants (14.2 ± 3.8 vs 11.1 ± 2.8 g 100 g^{-1}, and 190 ± 45 vs 149 ± 57 mm m^{-1}) ($p < 0.01$), while the water deficit under shallow-rooted plants is smaller than those under deep-rooted plants (73 ± 45 vs 114 ± 41 mm m^{-1}). This provides a good indication of the impact of vegetation.

3.2. Vertical variability of soil water

SW content varies with depth (Fig. 4). According to the vertical distributions of SW and CV, we defined the rapidly changing layer, active layer and relatively stable layer as depth profiles of 0–2 m, 2–5 m and below 5 m with shallow-rooted plants, but 0–2 m, 2–10 m and below 10 m with deep-rooted plants, respectively. SW content overall increases first and then decreases with depth. The mean SW content and storage in the relatively stable layer (14.5 ± 5.1 g 100 g^{-1}, and 192 ± 65 mm m^{-1}) are greater than those in the rapidly changing layer (11.8 ± 4.5 g 100 g^{-1}, and 158 ± 57 mm m^{-1}) and active layer (11.9 ± 5.1 g 100 g^{-1}, 158 ± 68 mm m^{-1}) ($p < 0.01$, Table 1). However, the water deficit in the relatively stable layer is smaller than the other two layers (72 ± 61 vs 105 ± 52 and 104 ± 57 mm m^{-1}).

The SW indices under shallow-rooted plants have similar vertical variability as all datasets. However, under deep-rooted plants, the mean SW content and storage are the highest at the relatively stable layer (13.7 ± 5.3 g 100 g^{-1}, and 182 ± 65 mm m^{-1}), intermediate in the rapidly changing layer (11.3 ± 4.5 g 100 g^{-1}, and 151 ± 56 mm m^{-1}), and the lowest in the active layer (10.3 ± 4.6 g 100 g^{-1}, and 139 ± 62 mm m^{-1}) ($p < 0.01$, Table 1). Furthermore, SW deficits under deep-rooted plants are larger than those under shallow-rooted plants in the three layers (80 ± 57 to 125 ± 45 vs 59 ± 59 to 93 ± 56 mm m^{-1}) ($p < 0.01$). With the plant age increasing, soil water reduction was getting severe in different soil layers, particularly in the active layer (Fig. S1), implying the differences in plant water consumption.

Vertical distributions of SW vary with climate. The SW curves gradually move to the right side approaching wetter conditions from arid to subhumid regions (Fig. 4). SW content and storage in the three soil layers in the subhumid climate are higher than those for the other two types of climate ($p < 0.01$). For different soil layers, SW content and storage in the relatively stable layer are larger than those in the rapidly changing layer and active layer under three types of climate (11.2 ± 4.3 to 15.2 ± 5.1 vs 7.4 ± 3.1 to 12.7 ± 4.3 g 100 g^{-1}, and 151 ± 45 to 200 ± 66 vs 99 ± 29 to 169 ± 53 mm m^{-1}) ($p < 0.01$).

3.3. Dominance of environmental factors

The correlation analysis provided little useful information since SW is significantly related to most environmental factors, which may be attributed to multicollinearity (Table S2). Consequently, we eliminated the multicollinearity to identify the factors dominating SW in the horizontal

Table 1
Statistics of mean soil water content, storage and deficit in different regions and soil layers across the Loess Plateau for 128 profiles.

Regions	Layers	SW, g 100 g^{-1}					SWS, mm m^{-1}					WD, mm m^{-1}				
		Min	Max	Aver	SDs	CVs	Min	Max	Aver	SDs	CVs	Min	Max	Aver	SDs	CVs
All profiles (N = 9289)	All profiles	5.0	21.1	12.3	4.4	0.36	63	308	164	59	0.36	−32	195	99	47	0.48
	Rapidly changing layer	1.5	24.8	11.8^{b}	4.5	0.38	48	302	158	57	0.36	−42	226	105	52	0.50
	Active layer	2.0	27.1	11.9^{b}	5.1	0.43	35	363	158	68	0.43	−61	256	104	57	0.54
	Relatively stable layer	2.3	29.4	14.5^{a}	5.1	0.35	55	342	192	65	0.34	−74	216	72	61	0.84
Shallow root (N = 3601)	All profiles	7.5	21.1	14.2^{A}	3.8	0.27	110	308	190	54	0.29	−32	169	73	45	0.62
	Rapidly changing layer	1.5	23.3	12.7^{Ab}	4.4	0.20	48	302	169	55	0.33	−42	226	93	54	0.58
	Active layer	3.5	23.9	12.7^{Ab}	4.5	0.35	53	324	170	61	0.36	−40	227	93	56	0.60
	Relatively stable layer	3.8	29.4	15.3^{Aa}	4.8	0.32	81	363	204	65	0.32	−74	211	59	59	0.99
Deep root (N = 5688)	All profiles	5.0	19.5	11.1^{B}	2.8	0.25	63	253	149	57	0.38	22	195	114	41	0.36
	Rapidly changing layer	2.9	24.8	11.3^{Bb}	4.5	0.39	48	277	151	56	0.37	7	223	112	50	0.45
	Active layer	2.0	26.3	10.3^{Bb}	4.6	0.45	35	313	139	62	0.45	−14	256	125	45	0.36
	Relatively stable layer	2.3	26.8	13.7^{Ba}	5.3	0.39	55	326	182	65	0.36	−38	216	80	57	0.71
Arid region (P1 < 200) (N = 350)	All profiles	5.4	10.3	8.6^{B}	1.8	0.21	68	129	107	23	0.21	133	195	155	23	0.15
	Rapidly changing layer	4.2	17.4	8.9^{Bb}	2.7	0.30	62	173	111	30	0.27	89	200	151	30	0.20
	Active layer	3.9	14.7	7.9^{Bb}	2.4	0.30	52	156	99	29	0.30	106	211	164	29	0.18
	Relatively stable layer	9.5	16.6	12.5^{Ba}	1.6	0.13	135	174	156	14	0.09	89	128	106	14	0.14
Semiarid region (200 < P2 < 400) (N = 1262)	All profiles	5.7	14.6	9.3^{B}	4.1	0.29	66	169	120	36	0.30	61	192	122	39	0.32
	Rapidly changing layer	1.5	19.1	7.4^{Cb}	3.1	0.42	48	236	100	40	0.40	2	226	142	50	0.35
	Active layer	2.0	20.3	8.5^{Bb}	3.7	0.44	35	296	116	52	0.45	−4	256	126	52	0.41
	Relatively stable layer	2.3	25.4	11.2^{Ba}	4.3	0.38	75	263	151	45	0.30	−34	216	109	61	0.56
Subhumid region (P3 > 400) (N = 7677)	All profiles	5.0	21.1	13.0^{A}	4.4	0.33	63	308	174	59	0.34	−32	185	92	46	0.51
	Rapidly changing layer	1.5	24.8	12.7^{Ab}	4.3	0.34	52	302	169	53	0.31	−42	217	97	50	0.51
	Active layer	2.4	27.1	12.6^{Ab}	5.1	0.40	42	363	168	68	0.40	−61	230	97	56	0.57
	Relatively stable layer	3.7	29.4	15.2^{Aa}	5.1	0.33	55	342	200	66	0.33	−74	208	65	59	0.91

Note: N is the number of soil samples. P is precipitation, mm. Min, Max and Aver represent minimum, maximum and average values, respectively. SDs and CVs represent standard deviation and coefficient of variation, respectively. SW, SWS and WD refer to soil water content, soil water storage and water deficit, respectively. P1, P2 and P3 refer to precipitation in arid, semiarid and subhumid regions, respectively. Different uppercases refer to significant differences under various plants or climates. Different lowercases represent significant differences among the three soil layers in different cases.

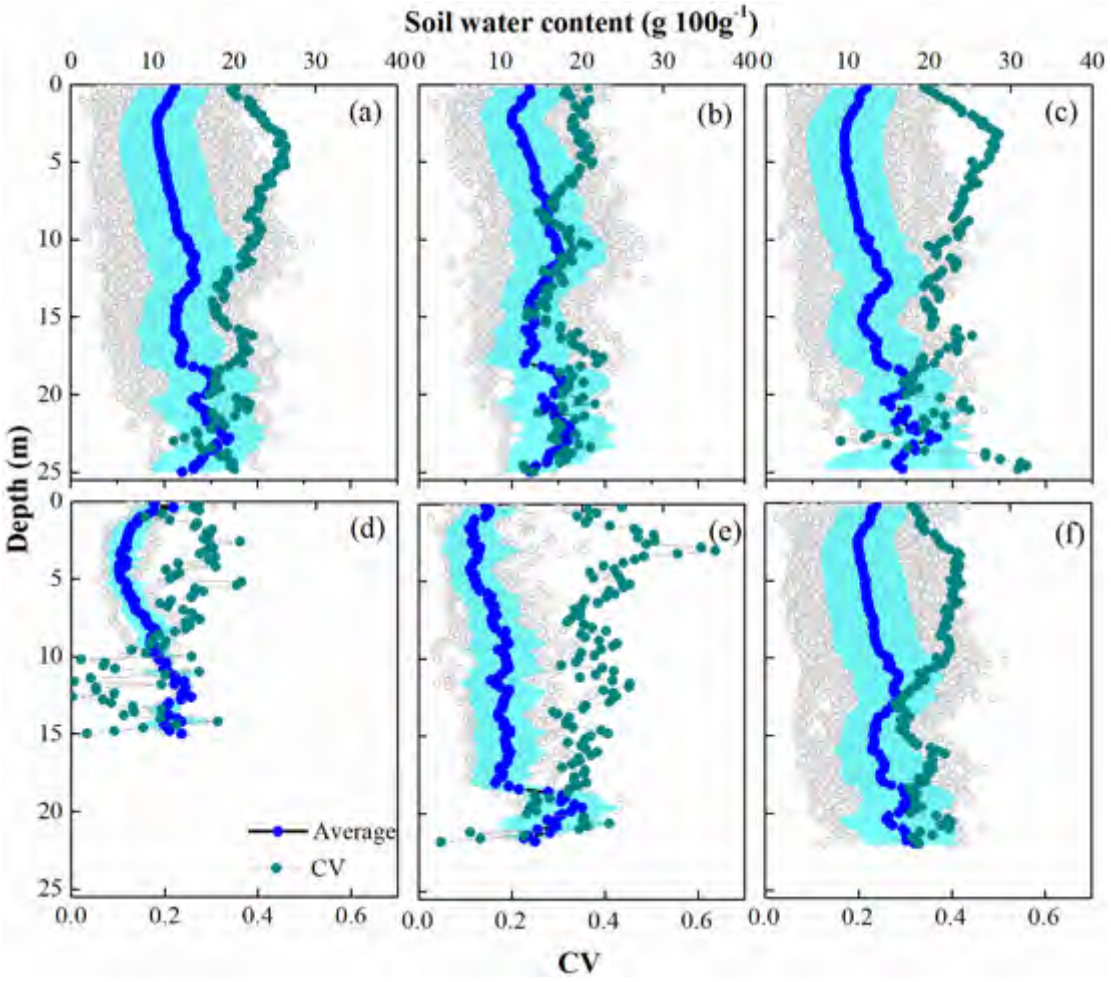

Fig. 4. Vertical distributions of soil water content. (a) Averaged over all sites. (b) Averaged over sites with shallow-rooted plants. (c) Averaged over sites with deep-rooted plants. (d) Averaged over sites in arid region (P1 < 200 mm), (e) Soil water profiles at sites in semiarid region (200 < P2 < 400 mm), (f) Soil water profiles at sites in subhumid region (P3 > 400 mm). Hollow gray circles refer to SW content of different soil profiles at all locations. Blue circles and shallow cyan filler represent the average soil water content and its standard deviation for all profiles. The green circles represent the coefficient of variation (CV). (a)–(f) share the same legend in (d). (For interpretation of the references to colour in this figure legend, the reader is referred to the web version of this article.)

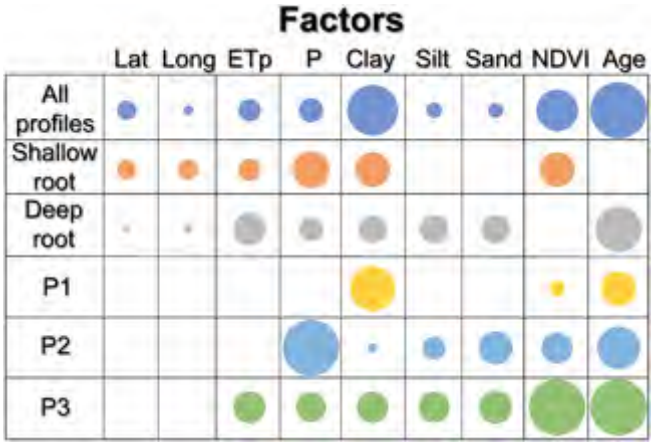

Fig. 5. Proportion of evidence (PoE) for each factor in the whole profiles, different rooted plants, and different climatic regions in the horizontal direction. P1, P2 and P3 represent the climate in arid (P1 < 200 mm), semiarid (200 < P2 < 400 mm) and subhuimid (P3 > 400 mm) region, respectively. Bubbles with different sizes represent the PoE value. Lat, Long, ETp, P, NDVI and Age represent latitude, longitude, potential evapotranspiration, precipitation, normalized difference vegetation index and plant age, respectively.

direction using multi-model analysis (Fig. 5 & Table S3). Plant age and soil clay content overall control SW with PoEs of 1.00 and 0.90, indicating the strong effects on SW. However, the influences of each factor vary with climate. Specifically, SW is dominated by soil clay content and plant age in arid regions (PoE ranged 0.61–0.79), precipitation and plant age in semiarid regions (0.76–1.00), but NDVI and plant age in subhumid regions (1.00), respectively. For plants with different root systems, SW under shallow-rooted plants is mostly controlled by precipitation, clay and NDVI (0.61–0.65); the corresponding variables with deep-rooted plants are plant age and potential evapotranspiration with PoE of 0.81 and 0.57.

Vertically, the PoEs of vegetation factors (0.88–1.00) are higher than those of soil properties (0.57–0.66) and climate factors (0.49–0.58) (Fig. 6 & Table S3). Specifically, plant age is the dominant driver for all profiles with the greatest explanatory power (1.00), followed by NDVI (0.88). The above two factors (i.e., plant age and NDVI) also dominate the active layers and relatively stable layers (1.00 and 0.88, and 1.00 and 0.78); however, plant age and soil sand content have the highest PoE in the rapidly changing layers (0.54 and 0.43). Under different plants, NDVI, precipitation and soil clay content (0.71–0.82) are the factors offering the best explanation for vertical variability of SW under shallow-rooted plants, while the corresponding variables are NDVI and plant age (1.00 and 0.82) under deep-rooted plants, respectively. In addition, different factors were further identified for different layers in the two root systems, i.e., precipitation and NDVI for rapidly changing layers, plant age and NDVI for the other layers in

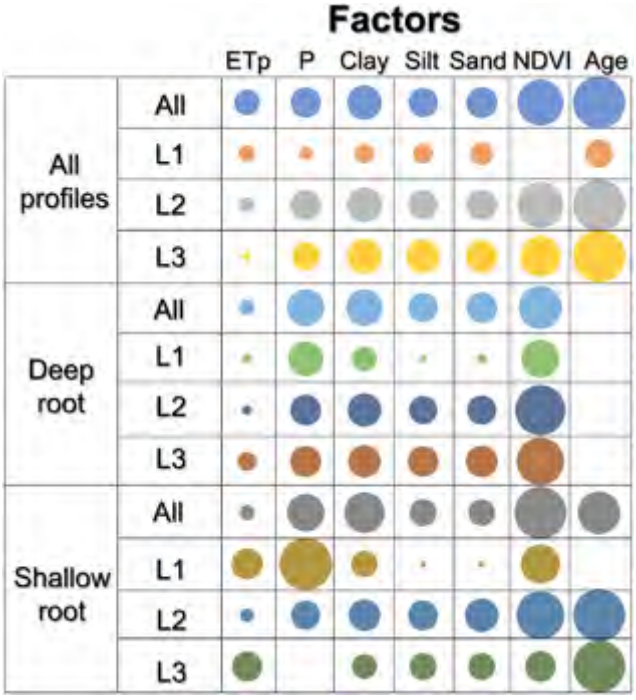

Fig. 6. Proportion of evidence (PoE) for each factor in the whole profiles and different rooted plants in the rapidly changing layer (L1), active layer (L2) and relatively stable layer (L3) in the vertical direction. Bubbles with different sizes represent the PoE value. P, NDVI and Age represent precipitation, normalized difference vegetation index and plant age, respectively.

the deep-rooted plants; while NDVI is the most important factor influencing SW of the three layers with high PoE (0.59–1.00) in the shallow-rooted plants.

3.4. Predicted models of SW

In this study, R^2_{adj} values remained almost constant once three or four factors were used for the model development (Fig. S2), indicating the appropriate number of predictors. With the number of predictors determined, the SW models were regressed (Table S4) and validated for different soil layers and vegetation systems (Fig. 7). Overall, the predicted and observed SW values were distributed along the 1:1 line, and the RMSE ranged 2.11–2.91 g 100 g^{-1} for horizontally averaged SW under different plant types, and 3.70–4.10 g 100 g^{-1} for vertical SW in different soil layers and/or different plants, respectively (Fig. 7). It indicated that the developed models are reliable in predicting SW for different soil layers and plants.

4. Discussion

4.1. How do environmental factors affect soil water variability?

SW varied horizontally with a downward gradient from the southeast to northwest in the Loess Plateau (Fig. 3). Although the horizontal variability of SW coincides with that of precipitation, the factors dominating SW were identified as plant age and soil clay content. This contradiction may be the result of the interactions of preferential factors in the agroforestry system (Liang et al., 2018; Wattenbach et al., 2007). The largely increased deep-rooted plants can deplete soil water because the root systems are being developed gradually as the stand ages (Bleby et al., 2010; Cui et al., 2019; Markewitz et al., 2010). The soil clay content determines the SW retention capacity (Markewitz et al., 2010; Qiao et al., 2018). As such, plant age and soil clay content combine to determine the water content in soils, suggesting that conserving SW is more important than increasing water inputs for SW management in the Loess Plateau.

Further, the driving factors for horizontally varied SW differ with climate. The factors dominating SW are soil clay content and plant age in arid regions, precipitation and plant age in semiarid regions, NDVI and plant age in subhumid regions, respectively (Fig. 5 & Table S3). Plant age, identified for each kind of climate, highlights the strong effects of root water uptake on SW (Beyer et al., 2018). The arid region has the largest evaporation but least precipitation with SW dominated by the ability of soil to conserve water (Gupta and Larson, 1979; Ravina and Magier, 1984). The semiarid region is sensitive to both the inputs and outputs of SW, which highlights the effects of precipitation (Seonghun et al., 2019; Welty and Zeng, 2018). With greater precipitation and better vegetation in subhumid regions, the stress from vegetation on SW is enhanced because of less biochemical limitation and photosynthetic advantage (Pace et al., 2021). The slight differences between the identified factors suggest the importance in the need for discriminating SW management for different climates (Gu et al., 2021).

Vertical distribution of SW is mainly influenced by the infiltration and redistribution of precipitation (Scott and Richard, 2015; Williams and Allman, 1969; Zhang et al., 1990). However, in this study, the vertical variability of SW is dominated by plant age and NDVI (Fig. 6 & Table S3), followed by such factors as soil type and climate. In the soil-plant-atmosphere system, plant growth is a primary mechanism of SW loss by transferring water to the atmosphere (Chang et al., 2020; Wang et al., 2013). The dominant effects of vegetation on vertical variability of SW suggest that root water uptake may overuse stored water but slow down water infiltration (Huang et al., 2018). For example, SW content is higher in the relatively stable layers than that in the rapidly changing layers and active layers (Table 1), which suggests depth influences root water consumption (Markewitz et al., 2010; Wang et al., 2013).

4.2. Why the SW variability is different under shallow- and deep-rooted plants?

The factors controlling SW variability differ with plant type because of their unique characteristics related to hydrology (Bouaziz et al., 2020; Dekker et al., 2007). Shallow-rooted plants can retain more water in soils because of small roots, weak water uptake capacity, high percolation and low evapotranspiration (Markewitz et al., 2010; Wang et al., 2012; Ye et al., 2019), and this can lead to spatially varied SW under different rainfall patterns (Sheil et al., 2019; Zhang et al., 2020b). In contrast, deep-rooted plants decrease SW by intense leaf interception and evaporation above the surface and strong root water uptake below the surface (Markewitz et al., 2010; Wang et al., 2012). In the Loess Plateau, with arid to subhumid climates, water inputs for SW are limited, but the water loss is large because of dry air and root water uptake (i.e., evapotranspiration). In particular, vegetation has a great influence on evapotranspiration, but the effects vary with plant type (Gu et al., 2021).

In this study, for both the horizontal and vertical direction of SW variability, precipitation, clay content and NDVI are the most important variables under shallow-rooted plants, while the corresponding variables under deep-rooted plants include plant age, NDVI and potential evapotranspiration (Figs. 5 & 6, Table S3). Under shallow-rooted plants, water inputs from precipitation, water conservation from clay content, and water loss from vegetation combine to control SW; however, under deep-rooted plants, the factors related to vegetation have overwhelming importance over other factors since plant age and NDVI are related directly to vegetation while evapotranspiration is related indirectly to vegetation (Asokan et al., 2010; Gu et al., 2021; Zhou et al., 2015). Consequently, deep-rooted plants alter SW cycling more than under shallow-rooted plants, highlighting the vegetation effects on SW in the Loess Plateau.

Water deficits were detected in the arid and semiarid regions under shallow-rooted plants, while these deficits exist across the entire study area for the deep-rooted plants (Fig. 3 & Table 1), implying the balance between plant water requirements and water availability varies with climate and plant type. Particularly, compared with shallow-rooted plants, trees with developed root systems in the Loess Plateau, were found to reduce SW by 11%, 17.3% and 4% in the rapidly changing layers, active layers

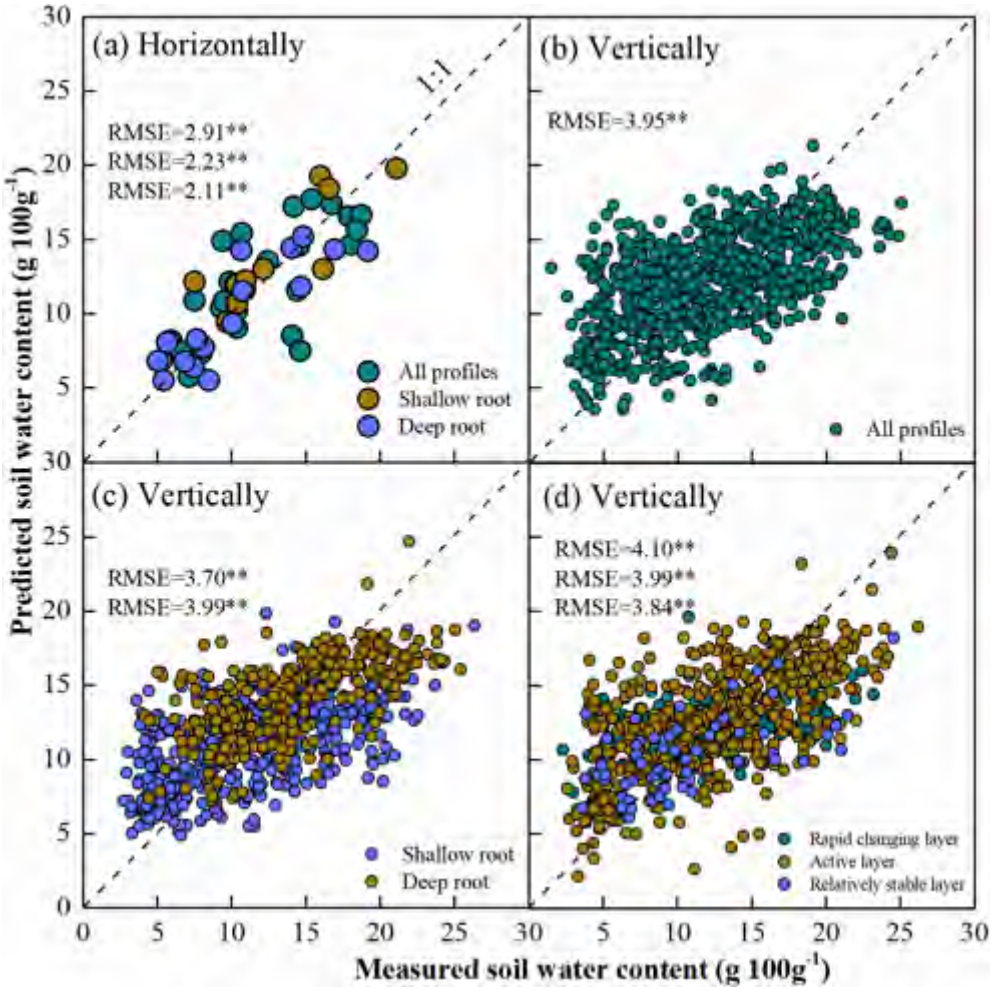

Fig. 7. Scatter plots of predicted horizontal SW content in all profiles and different rooted plants (a), predicted vertical SW content in all profiles (b), different rooted plants (c) and different soil layers (d). The model performances for predicting SW content are also showed in Table S3.

and stable layers, respectively (Table 1), implying the importance of tree impacts on soil ecosystem services. Alternatively, from the perspective of sustainability of water resources, deep-rooted plants can be used for revegetation if they can be managed according to their stand ages. Specifically, soil water depletion mainly occurs in the active layers for plants with stand ages <20 years while it can be detected in the relatively stable layers for plants with stand ages >30 years (Fig. S1).

According to previous studies, plant age is positively related to root length density and maximum root depth (Li et al., 2019a; Zhang et al., 2021), while our previous studies demonstrated that older plants lead to larger water deficits by absorbing old bound water which stored in soil with strong water-water binding and weak movement (Li et al., 2018; Zhang et al., 2017). SW content is negatively correlated with plant age (Fig. 8, $p < 0.01$), which further confirms the chronic depletion of SW because of gradually developing root systems with increasing age (Chen et al., 2008). These conclusions provide a reasonable explanation of the mechanism of the role of plants and related factors which influence SW for deep-rooted plants. The resultant water deficit, in turn, affects the balance of the agroforestry system, such as vegetation degradation; many small old trees exist in the Loess Plateau since limited available water in soil cannot meet the large water requirements of plants (Liu et al., 2018).

4.3. Uncertainties and implications

This study identified the dominant factors of SW in horizontal and vertical directions by combining the multimodel inference approach and stepwise regression analysis; however, the potential application of established models should consider data availability. First, this study employed the tritium peak method for SW aging at different depths, and then

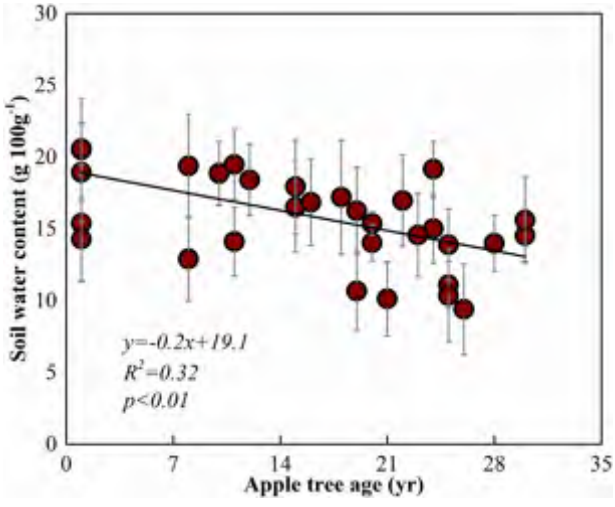

Fig. 8. Fitted relationships between SW and apple tree age. Red circles are averaged SW contents of each profile, the light gray lines represent the error bars. The black line is the fitting line between SW contents and apple tree ages. (For interpretation of the references to colour in this figure legend, the reader is referred to the web version of this article.)

incorporated the corresponding historical climate information for SW prediction model development. Although it is not possible for each site to use the tritium profile for SW dating, other alternative methods can be used for this purpose, such as chloride mass balance (Phillips et al., 1988). All the regressed equations include precipitation, indicating the overwhelming importance of precipitation in predicting SW (Dekker et al., 2007; Lazo et al., 2019; Wang et al., 2020; Yuan et al., 2021; Zhang et al., 2020a). This implies that it may be more accurate to develop models for each climate type. This will require future investigation once enough SW data is available for different climates. This study used NDVI data with a 250-m resolution for each sampling site, which may make it difficult to distinguish the NDVI values of different sites at the same location. However, it is still representative when analyzing SW variability for the large horizontal domain. Finally, to reveal the effects of vegetation on SW, the parameterization of vegetation should be conducted for large-scale SW prediction. For example, the plant parameters related to stand age or root density should be interpreted at fine spatial resolution.

The main variations in SW after tree planting in the Loess Plateau are the significant reduction in SW storage, which could cause degradation for the restored ecosystem (Zhang et al., 2018). The effects of vegetation change on SW provide insights for vegetation adjustments to avoid the depletion of water resources (Feng et al., 2016; Kumar et al., 2020). Specifically, selecting appropriate tree species should be taken into account. Then, studying the effects of vegetation density and integrated cultivation (mixed vegetation) on soil hydrological processes can guide the conservation of soil moisture in an agroforestry system. Further, model simulations and empirical tests should be conducted to find a vegetation pattern that maintains a balance between limited water resources and plant water demand for a revegetation project.

5. Conclusions

Understanding the mechanisms behind spatially and temporally varied SW is important to balance hydrological and ecological systems. This study explored this issue by relating different environmental factors to SW to determine their dominance in the Loess Plateau. SW content and storage increased along the northwest-southeast direction, while SW deficits decreased under shallow-rooted systems but there was little difference with deep-rooted plants. SW content and storage in the deep layers are greater than those in shallow layers. The most influential factors are plant age and soil clay content in the horizontal direction, while plant age and NDVI are important in the vertical direction. However, SW in different climatic regions and/or plants is dominated by a variety of environmental factors. This study highlights the importance of understanding the effect of vegetation change on the mechanisms of SW variability in an agroforestry ecosystem.

CRediT authorship contribution statement

Yanan Huang: Conceptualization, Methodology, Investigation, Validation, Writing – original draft, Formal analysis, Writing – review & editing. **Bingbing Li:** Validation, Formal analysis, Visualization. **Asim Biswas:** Writing – review & editing. **Zhi Li:** Conceptualization, Funding acquisition, Writing – review & editing, Supervision, Methodology.

Declaration of competing interest

The authors declare that they have no competing interests.

Acknowledgements

This research was jointly supported by National Natural Science Foundation of China (42071043) and Chinese Universities Scientific Fund (2452020002). With thanks to all the authors for their data and relevant research work involved in this study.

Appendix A. Supplementary data

Supplementary data to this article can be found online at https://doi.org/10.1016/j.scitotenv.2021.152172.

References

Allison, G., Hughes, M., 1978. The use of environmental chloride and tritium to estimate total recharge to an unconfined aquifer. Aust. J. Soil Res. 16, 181–195. https://doi.org/10.1016/0022-1694(75)90006-2.

An, W., Li, Z., Wang, S., Wu, X., Lu, Y., Liu, G., et al., 2017. Exploring the effects of the "Grain for green" program on the differences in soil water in the semi-arid loess plateau of China. Ecol. Eng. 107, 144–151. https://doi.org/10.1016/j.ecoleng.2017.07.017.

Asokan, S.M., Jerker, J., Destouni, G., 2010. Vapor flux by evapotranspiration: effects of changes in climate, land use, and water use. J. Geophys. Res. 115, D24102. https://doi.org/10.1029/2010jd014417.

Beyer, M., Hamutoko, J.T., Wanke, H., Gaj, M., Koeniger, P., 2018. Examination of deep root water uptake using anomalies of soil water stable isotopes, depth-controlled isotopic labeling and mixing models. J. Hydrol. 566, 122–136. https://doi.org/10.1016/j.jhydrol.2018.08.060.

Biggelaar, C.D., Lal, R., Wiebe, K., Breneman, V., 2003. The global impact of soil erosion on productivity: I: absolute and relative erosion-induced yield losses. Adv. Agron. 81, 1–48. https://doi.org/10.1016/S0065-2113(03)81001-5.

Bleby, T.M., McElrone, A.J., Jackson, R.B., 2010. Water uptake and hydraulic redistribution across large woody root systems to 20 m depth. Plant Cell Environ. 33, 2132–2148. https://doi.org/10.1111/j.1365-3040.2010.02212.x.

Bosch, D.D., Lakshmi, V., Jackson, T.J., Choi, M., Jacobs, J.M., 2006. Large scale measurements of soil moisture for validation of remotely sensed data: Georgia soil moisture experiment of 2003. J. Hydrol. 323, 120–137. https://doi.org/10.1016/j.jhydrol.2005.08.024.

Bouaziz, L.J.E., Steele-Dunne, S.C., Schellekens, J., Weerts, A.H., Stam, J., Sprokkereef, E., et al., 2020. Improved understanding of the link between catchment-scale vegetation accessible storage and satellite-derived soil water index. Water Resour. Res. 56, e2019WR026365. https://doi.org/10.1029/2019wr026365.

Chang, C., Yeh, H., Chuang, M., 2020. Quantification of temporal variability of vertical soil moisture movement through an unsaturated zone. Adv. Water Resour. 145, 103752. https://doi.org/10.1016/j.advwatres.2020.103752.

Chen, H., Shao, M., Li, Y., 2008. Soil desiccation in the loess plateau of China. Geoderma 143, 91–100. https://doi.org/10.1016/j.geoderma.2007.10.013.

Cleverly, J., Eamus, D., Coupe, N.R., Chen, C., Maes, W.H., Li, L.H., et al., 2016. Soil moisture controls on phenology and productivity in a semi-arid critical zone. Sci. Total Environ. 568, 1227–1237. https://doi.org/10.1016/j.scitotenv.2016.05.142.

Cui, Z., Wu, G.-L., Huang, Z., Liu, Y., 2019. Fine roots determine soil infiltration potential than soil water content in semi-arid grassland soils. J. Hydrol. 578, 124023. https://doi.org/10.1016/j.jhydrol.2019.124023.

da Silva, A.P., Nadler, A., Kay, B.D., 2001. Factors contributing to temporal stability in spatial patterns of water content in the tillage zone. Soil Till Res. 58, 207–218. https://doi.org/10.1016/S0167-1987(00)00169-0.

Dekker, S.C., Rietkerk, M.A.X., Bierkens, M.F.P., 2007. Coupling microscale vegetation–soil water and macroscale vegetation–precipitation feedbacks in semiarid ecosystems. Glob. Chang. Biol. 13, 671–678. https://doi.org/10.1111/j.1365-2486.2007.01327.x.

Duan, Q., Ajami, N.K., Gao, X., Sorooshian, S., 2007. Multi-model ensemble hydrologic prediction using bayesian model averaging. Adv. Water Resour. 30, 1371–1386. https://doi.org/10.1016/j.advwatres.2006.11.014.

Famiglietti, J.S., Rudnicki, J.W., Rodell, M., 1998. Variability in surface moisture content along a hillslope transect: Rattlesnake HillTexas. J Hydrol. 210, 259–281. https://doi.org/10.1016/S0022-1694(98)00187-5.

Feng, X., Fu, B., Piao, S., Wang, S., Ciais, P., Zeng, Z., et al., 2016. Revegetation in China's loess plateau is approaching sustainable water resource limits. Nat. Clim. Chang. 6, 1019–1022. https://doi.org/10.1038/nclimate3092.

Feng, X., Li, J., Cheng, W., Fu, B., Wang, Y., Lü, Y., et al., 2017. Evaluation of AMSR-E retrieval by detecting soil moisture decrease following massive dryland re-vegetation in the loess plateauChina. Remote Sens. Environ. 196, 253–264. https://doi.org/10.1016/j.rse.2017.05.012.

Fenicia, F., Savenije, H.H.G., Matgen, P., Pfister, L., 2008. Understanding catchment behavior through stepwise model concept improvement. Water Resour. Res. 44, W01402. https://doi.org/10.1029/2006wr005563.

Gao, L., Shao, M., 2012. Temporal stability of shallow soil water content for three adjacent transects on a hillslope. Agric. Water Manag. 110, 41–54. https://doi.org/10.1016/j.agwat.2012.03.012.

Gao, X., Zhao, X., Wu, P., Brocca, L., Zhang, B., 2016. Effects of large gullies on catchment-scale soil moisture spatial behaviors: a case study on the loess plateau of China. Geoderma 261, 1–10. https://doi.org/10.1016/j.geoderma.2015.07.001.

Glüer, C.C., Blake, G., Lu, Y., Blunt, B.A., Jergas, M., Genant, H.K., 1995. Accurate assessment of precision errors: how to measure the reproducibility of bone densitometry techniques. Osteoporosis Int. 5, 262–270. https://doi.org/10.1007/BF01774016.

Gong, Z., Zhang, G., 2007. Chinese soil taxonomy: a milestone of soil classification in China. Science Foundation in China 15, 41–45.

Grassini, P., You, J., Hubbard, K.G., Cassman, K.G., 2010. Soil water recharge in a semi-arid temperate climate of the central U.S. Great Plains. Agric. Water Manage. 97, 1063–1069. https://doi.org/10.1016/j.agwat.2010.02.019.

Green, J.K., Seneviratne, S.I., Berg, A.M., Findell, K.L., Hagemann, S., Lawrence, D.M., et al., 2019. Large influence of soil moisture on long-term terrestrial carbon uptake. Nature 565, 476–479. https://doi.org/10.1038/s41586-018-0848-x.

Gu, C., Tang, Q., Zhu, G., Ma, J., Gu, C., Zhang, K., et al., 2021. Discrepant responses between evapotranspiration- and transpiration-based ecosystem water use efficiency to interannual precipitation fluctuations. Agric. For. Meteorol. 303, 108385. https://doi.org/10.1016/j.agrformet.2021.108385.

Guillod, B.P., Orlowsky, B., Miralles, D.G., Teuling, A.J., Seneviratne, S.I., 2015. Reconciling spatial and temporal soil moisture effects on afternoon rainfall. Nat. Commun. 6, 6443. https://doi.org/10.1038/ncomms7443.

Gupta, S.C., Larson, W.E., 1979. Estimating soil water retention characteristics from particle size distribution, organic matter percent, and bulk density. Water Resour. Res. 15, 1633–1635. https://doi.org/10.1029/WR015i006p01633.

Hargreaves, George H., 1994. Defining and using reference evapotranspiration. J. Irrig. Drain. Eng. 120, 1132–1139. https://doi.org/10.1061/(ASCE)0733-9437(1994)120:6(1132).

Hendrickx, J.M.H., Wierenga, P.J., Nash, M.S., 1990. Variability of soil water tension and soil water content. Agric. Water Manag. 18, 135–148. https://doi.org/10.1016/0378-3774(90)90026-U.

Hu, W., Si, B.C., 2013. Soil water prediction based on its scale-specific control using multivariate empirical mode decomposition. Geoderma 193–194, 180–188. https://doi.org/10.1016/j.geoderma.2012.10.021.

Hu, W., Si, B.C., 2014. Revealing the relative influence of soil and topographic properties on soil water content distribution at the watershed scale in two sites. J. Hydrol. 516, 107–118. https://doi.org/10.1016/j.jhydrol.2013.10.002.

Huang, Y., Chang, Q., Li, Z., 2018. Land use change impacts on the amount and quality of recharge water in the loess tablelands of China. Sci. Total Environ. 628–629, 443–452. https://doi.org/10.1016/j.scitotenv.2018.02.076.

Jensen, D.T., Hargreaves, G.H., Temesgen, B., Allen, R.G., 1997. Computation of ETo under nonideal conditions. J. Irrig. Drain. Eng. 123, 394–400. https://doi.org/10.1061/(ASCE)0733-9437(1997)123:5(394).

Jian, S., Zhao, C., Fang, S., Yu, K., 2015. Effects of different vegetation restoration on soil water storage and water balance in the Chinese loess plateau. Agric. For. Meteorol. 206, 85–96. https://doi.org/10.1016/j.agrformet.2015.03.009.

Jiao, Q., Li, R., Wang, F., Mu, X., Li, P., An, C., 2016. Impacts of re-vegetation on surface soil moisture over the Chinese loess plateau based on remote sensing datasets. Remote Sens-basel. 8, 156. https://doi.org/10.3390/rs8020156.

Jing, Z., Cheng, J., Chen, A., 2013. Assessment of vegetative ecological characteristics and the succession process during three decades of grazing exclusion in a continental steppe grassland. Ecol. Eng. 57, 162–169. https://doi.org/10.1016/j.ecoleng.2013.04.035.

Jung, M., Reichstein, M., Ciais, P., Seneviratne, S., Sheffield, J., Goulden, M., et al., 2010. Recent decline in the global land evapotranspiration trend due to limited moisture supply. Nature 467. https://doi.org/10.1038/nature09396.

Kumar, R., Bhatnagar, P.R., Kakade, V., Dobhal, S., 2020. Tree plantation and soil water conservation enhances climate resilience and carbon sequestration of agro ecosystem in semi-arid degraded ravine lands. Agric. For. Meteorol. 282–283, 107857. https://doi.org/10.1016/j.agrformet.2019.107857.

Lal, R., 2001. Soil degradation by erosion. Land Degrad. Dev. 12, 519–539. https://doi.org/10.1002/ldr.472.

Lazo, P.X., Mosquera, G.M., McDonnell, J.J., Crespo, P., 2019. The role of vegetation, soils, and precipitation on water storage and hydrological services in Andean paramo catchments. J. Hydrol. 572, 805–819. https://doi.org/10.1016/j.jhydrol.2019.03.050.

Li, Y., Huang, M., 2008. Pasture yield and soil water depletion of continuous growing alfalfa in the loess plateau of China. AgricEcosyst. Environ. 124, 24–32. https://doi.org/10.1016/j.agee.2007.08.007.

Li, H., Si, B., Li, M., 2018. Rooting depth controls potential groundwater recharge on hillslopes. J of Hydrol. 564, 164–174. https://doi.org/10.1016/j.jhydrol.2018.07.002.

Li, H., Si, B., Wu, P., McDonnell, J.J., 2019a. Water mining from the deep critical zone by apple trees growing on loess. Hydrol. Process. 33, 320–327. https://doi.org/10.1002/hyp.13346.

Li, Z., Jasechko, S., Si, B., 2019b. Uncertainties in tritium mass balance models for groundwater recharge estimation. J. Hydrol. 571, 150–158.. https://doi.org/10.1016/j.jhydrol.2019.01.030.

Li, Z., Ma, J., Song, L., Gui, J., Xue, J., Zhang, B., et al., 2020. Investigation of soil water hydrological process in the permafrost active layer using stable isotopes. Hydrol. Process. 34, 2810–2822 https://doi.org/410.1002/hyp.13765.

Liang, H., Xue, Y., Li, Z., Wang, S., Wu, X., Gao, G., et al., 2018. Soil moisture decline following the plantation of Robinia pseudoacacia forests: evidence from the loess plateau. For. Ecol. Manag. 412, 62–69. https://doi.org/10.1016/j.foreco.2018.01.041.

Liu, Y., Miao, H.-T., Huang, Z., Cui, Z., He, H., Zheng, J., et al., 2018. Soil water depletion patterns of artificial forest species and ages on the loess plateau (China). For. Ecol. Manag. 417, 137–143. https://doi.org/10.1016/j.foreco.2018.03.005.

Maddock, Iii T., 1976. A drawdown prediction model based on regression analysis. Water Resour. Res. 12, 818–822. https://doi.org/10.1029/WR012i004p00818.

Markewitz, D., Devine, S., Davidson, E.A., Brando, P., Nepstad, D.C., 2010. Soil moisture depletion under simulated drought in the Amazon: impacts on deep root uptake. New Phytol. 187, 592–607. https://doi.org/10.1111/j.1469-8137.2010.03391.x.

Mei, X.M., Ma, L., Zhu, Q.K., Li, B., Zhang, D., Liu, H.F., et al., 2019. The variability in soil water storage on the loess hillslopes in China and its estimation. Catena 172, 807–818. https://doi.org/10.1016/j.catena.2018.09.045.

Melliger, J.J., Niemann, J.D., 2010. Effects of gullies on space–time patterns of soil moisture in a semiarid grassland. J. Hydrol. 389, 289–300. https://doi.org/10.1016/j.jhydrol.2010.06.006.

Mohan, C., Western, A.W., Wei, Y., Saft, M., 2018. Predicting groundwater recharge for varying land cover and climate conditions – a global meta-study. Hydrol. Earth Syst. Sci. 22, 2689–2703. https://doi.org/10.5194/hess-22-2689-2018.

Namdar-Khojasteh, D., Shorafa, M., Heidari, A., 2012. Estimating soil water content from permittivity for different mineralogies and bulk densities. Soil Sci. Soc. Am. J. 76, 1149–1158. https://doi.org/10.2136/sssaj2011.0144.

Nielsen, D.R., Biggar, J.W., Erh, K.T., 1973. Spatial variability of field-measured soil-water properties. Hilgardia 42, 214–259. https://doi.org/10.3733/hilg.v42n07p215.

Pace, G., Gutierrez-Canovas, C., Henriques, R., Boeing, F., Cassio, F., Pascoal, C., 2021. Remote sensing depicts riparian vegetation responses to water stress in a humid Atlantic region. Sci. Total Environ. 772, 145526. https://doi.org/10.1016/j.scitotenv.2021.145526.

Peng, S., Ding, Y., Liu, W., Li, Z., 2019. 1 km monthly temperature and precipitation dataset for China from 1901 to 2017. Earth Syst. Sci. Data 11, 1931–1946. https://doi.org/10.5194/essd-11-1931-2019.

Perry, M.A., Niemann, J.D., 2007. Analysis and estimation of soil moisture at the catchment scale using EOFs. J. Hydrol. 334, 388–404. https://doi.org/10.1016/j.jhydrol.2006.10.014.

Petropoulos, G.P., Ireland, G., Barrett, B., 2015. Surface soil moisture retrievals from remote sensing: current status, products & future trends. PhysChem. Earth, Parts A/B/C 83–84, 36–56. https://doi.org/10.1016/j.pce.2015.02.009.

Phillips, F.M., Mattick, J.L., Duval, T.A., Elmore, D., Kubik, P.W., 1988. Chlorine 36 and tritium from nuclear weapons fallout as tracers for long-term liquid and vapor movement in desert soils. Water Resour. Res. 24, 1877–1891. https://doi.org/10.1029/WR024i011p01877.

Piper, C.S., 1966. Soil and Plant Analysis. Hans Publishers, Bombay.

Poeter, E., Anderson, D., 2005. Multimodel ranking and inference in ground water modeling. Ground Water 43, 597–605. https://doi.org/10.1111/j.1745-6584.2005.0061.x.

Qiao, J., Zhu, Y., Jia, X., Huang, L., Shao, M.A., 2018. Factors that Influence the Vertical Distribution of Soil Water Content in the Critical Zone on the Loess Plateau. China. Vadose Zone J 17, 170196. https://doi.org/10.2136/vzj2017.11.0196.

Qu, W., Bogena, H.R., Huisman, J.A., Vanderborght, J., Schuh, M., Priesack, E., et al., 2015. Predicting subgrid variability of soil water content from basic soil information. Geophys. Res. Lett. 42, 789–796. https://doi.org/10.1002/2014GL062496.

Ravina, I., Magier, J., 1984. Hydraulic Conductivity and Water Retention of Clay Soils Containing Coarse Fragments. Soil Sci. Soc. Am. J. 48, 736–740. https://doi.org/10.2136/sssaj1984.03615995004800040008x.

Rodriguez-Iturbe, I., D'Odorico, P., Porporato, A., Ridolfi, L., 1999. On the spatial and temporal links between vegetation, climate, and soil moisture. Water Resour. Res. 35, 3709–3722. https://doi.org/10.1029/1999WR900255.

Sándor, R., Iovino, M., Lichner, L., Alagna, V., Forster, D., Fraser, M., et al., 2021. Impact of climate, soil properties and grassland cover on soil water repellency. Geoderma 383, 114780. https://doi.org/10.1016/j.geoderma.2020.114780.

Sandrin, L., Fourquet, B., Hasquenoph, J.-M., Yon, S., Fournier, C., Mal, F., et al., 2003. Transient elastography: a new noninvasive method for assessment of hepatic fibrosis. Ultrasound in Med. Biol. 29, 1705–1713. https://doi.org/10.1016/j.ultrasmedbio.2003.07.001.

Scott, J., Richard, G.T., 2015. Intensive rainfall recharges tropical groundwaters. Environ. Res. Lett. 10, 124015.

Seonghun, J., Otsuki, K., Moein, F., 2019. Relationship between stand structures and rainfall partitioning in dense unmanaged Japanese cypress plantations. J. Agric. Meteorol. 75, 92–102. https://doi.org/10.2480/agrmet.D-18-00030.

Shao, X., Wang, Y., Bi, L., Yuan, Y., Su, X., Mo, J., 2009. Study on soil water characteristics of tobacco fields based on canonical correlation analysis. Water Sci. Eng. 2, 79–86. https://doi.org/10.3882/j.issn.1674-2370.2009.02.009.

Sheil, D., Bargués-Tobella, A., Ilstedt, U., Ibisch, P.L., Makarieva, A., McAlpine, C., et al., 2019. Forest restoration: Transformative trees. Science 366, 316. https://doi.org/10.1126/science.aay7309.

Shi, H., Shao, M., 2000. Soil and water loss from the Loess Plateau in China. J. Arid Environ. 45, 9–20. https://doi.org/10.1006/jare.1999.0618.

Stonestrom, D.A., Scanlon, B.R., Zhang, L., 2009. Introduction to special section on Impacts of Land Use Change on Water Resources. Water Resour. Res. 45, 160–169. https://doi.org/10.1029/2009WR007937.

Su, B., Shangguan, Z., 2019. Decline in soil moisture due to vegetation restoration on the Loess Plateau of China. Land Degrad. Dev. 30, 290–299.

Sun, N.-Z., Yang, S.-L., Yeh, W.W.G., 1998. A proposed stepwise regression method for model structure identification. Water Resour. Res. 34, 2561–2572. https://doi.org/10.1029/98WR01860.

ter Braak, C.J.F., Verdonschot, P.F.M., 1995. Canonical correspondence analysis and related multivariate methods in aquatic ecology. Aquat. Sci. 57, 255–289. https://doi.org/10.1007/BF00877430.

Tite, M.S., Linington, R.E., 1975. Effect of climate on the magnetic susceptibility of soils. Nature 256, 565–566. https://doi.org/10.1038/256565a0.

Vidic, N.J., Singer, M.J., Verosub, K.L., 2004. Duration dependence of magnetic susceptibility enhancement in the Chinese loess–palaeosols of the past 620 ky. Palaeogeogr Palaeoecol. 211, 271–288. https://doi.org/10.1016/j.palaeo.2004.05.012.

Wang, S., Fu, B.J., Gao, G.Y., Yao, X.L., Zhou, J., 2012. Soil moisture and evapotranspiration of different land cover types in the Loess Plateau. China. Hydrol. Earth Syst. Sci. 16, 2883–2892. https://doi.org/10.5194/hess-16-2883-2012.

Wang, Y., Shao, M., Liu, Z., 2013. Vertical distribution and influencing factors of soil water content;within 21-m profile on the Chinese Loess Plateau. Geoderma 193, 300–310. https://doi.org/10.1016/j.geoderma.2012.10.011.

Wang, X., Zhu, D., Wang, Y., Wei, X., Ma, L., 2015. Soil water and root distribution under jujube plantations in the semiarid Loess Plateau regionChina. Plant Growth Regul. 77, 21–31. https://doi.org/10.1007/s10725-015-0031-4.

Wang, Y., Shao, M.A., Sun, H., Fu, Z., Fan, J., Hu, W., 2020. Response of deep soil drought to precipitation, land use and topography across a semiarid watershed. Agri. Forest Meteorol. 282-283, 107866. https://doi.org/10.1016/j.agrformet.2019.107866.

Wattenbach, M., Zebisch, M., Hattermann, F., Gottschalk, P., Goemann, H., Kreins, P., et al., 2007. Hydrological impact assessment of afforestation and change in tree-species composition – A regional case study for the Federal State of Brandenburg (Germany). J. Hydrol. 346, 1–17. https://doi.org/10.1016/j.jhydrol.2007.08.005.

Welty, J., Zeng, X., 2018. Does soil moisture affect warm season precipitation over the southern great plains? Geophys. Res. Lett. 45, 7866–7873. https://doi.org/10.1029/2018GL078598.

Western, A.W., Zhou, S., Grayson, R.B., McMahon, T.A., Blöschl, G., Wilson, D.J., 2004. Spatial correlation of soil moisture in small catchments and its relationship to dominant spatial hydrological processes. J. Hydrol. 286, 113. https://doi.org/10.1016/j.jhydrol.2003.09.014.

Williams, R.E., Allman, D.W., 1969. Factors affecting infiltration and recharge in a loess covered basin. J. Hydrol. 8, 265–281. https://doi.org/10.1016/0022-1694(69)90002-X.

Wilson, D.J., Western, A.W., Grayson, R.B., 2005. A terrain and data-based method for generating the spatial distribution of soil moisture. Adv. Water Resour. 28, 43–54. https://doi.org/10.1016/j.advwatres.2004.09.007.

Yao, Y., Wang, X., Zeng, Z., Liu, Y., Peng, S., Zhu, Z., et al., 2016. The Effect of Afforestation on Soil Moisture Content in Northeastern China. PLoS One 11, e0160776. https://doi.org/10.1371/journal.pone.0160776.

Ye, L., Fang, L., Shi, Z., Deng, L., Tan, W., 2019. Spatio-temporal dynamics of soil moisture driven by 'Grain for Green' program on the Loess PlateauChina. Agric. Ecosyst. Environ. 269, 204–214. https://doi.org/10.1016/j.agee.2018.10.006.

Yuan, G., Zhang, L., Liu, Y., 2021. Impacts of soil moisture and atmospheric moisture transport on the precipitation in two typical regions of China. Atmos. Res. 247, 105151. https://doi.org/10.1016/j.atmosres.2020.105151.

Zhang, M., Wei, X., 2021. Deforestation, forestation, and water supply. Science 371, 990–991. https://doi.org/10.1126/science.abe7821.

Zhang, Z., Liu, F., Zhang, H., Liu, E., 1990. Study of soil water movement and recharge rate of rainfall infiltration in aeration zone of loess by measuring natural tritium. Hydrogeol. Eng. Geol. 5–8.

Zhang, Y., Deng, L., Yan, W., Shangguan, Z., 2016. Interaction of soil water storage dynamics and long-term natural vegetation succession on the Loess Plateau, China. Catena 137, 52–60. https://doi.org/10.1016/j.catena.2015.08.016.

Zhang, Z.Q., Evaristo, J., Li, Z., Si, B.C., McDonnell, J.J., 2017. Tritium analysis shows apple trees may be transpiring water several decades old. Hydrol. Process. 31, 1196–1201. https://doi.org/10.1002/hyp.11108.

Zhang, Z., Li, M., Si, B., Feng, H., 2018. Deep rooted apple trees decrease groundwater recharge in the highland region of the Loess PlateauChina. Sci. Total Environ. 622–623, 584–593. https://doi.org/10.1016/j.scitotenv.2017.11.230.

Zhang, C., Wang, Y., Jia, X., Shao, M.A., An, Z., 2020. Variations in capacity and storage of plant-available water in deep profiles along a revegetation and precipitation gradient. J. Hydrol. 581, 124401. https://doi.org/10.1016/j.jhydrol.2019.124401.

Zhang, Q., Wei, W., Chen, L., Yang, L., Luo, Y., Cai, A., 2020b. Plant traits in influencing soil moisture in semiarid grasslands of the Loess PlateauChina. Sci. Total Environ. 718, 137355. https://doi.org/10.1016/j.scitotenv.2020.137355.

Zhang, J., Li, Y., Yang, T., Liu, D., Liu, X., Jiang, N., 2021. Spatiotemporal variation of moisture in rooted-soil. Catena 200, 105144. https://doi.org/10.1016/j.catena.2021.105144.

Zhou, G., Wei, X., Chen, X., Zhou, P., Liu, X., Xiao, Y., et al., 2015. Global pattern for the effect of climate and land cover on water yield. Nat. Commun. 6, 5918. https://doi.org/10.1038/ncomms6918.

Zhu, X., Li, Y., Peng, X., Zhang, S., 1983. Soils of the loess region in China. Geoderma 29, 237–255. https://doi.org/10.1016/0016-7061(83)90090-3.

Ziadat, F.M., Taimeh, A.Y., 2013. Effect of rainfall intensity, slope, land use and antecedent soil moisture on soil erosion in an arid environment. Land Degrad. Dev. 24, 582–590. https://doi.org/10.1002/ldr.2239.